

Mechanisms of Cardiac and Renal Dysfunction in Patients Dying of Sepsis

Osamu Takasu^{1*}, Joseph P. Gaut^{2*}, Eizo Watanabe³, Kathleen To³, R. Eliot Fagley¹, Brian Sato¹, Steve Jarman³, Igor R. Efimov⁴, Deborah L. Janks⁴, Anil Srivastava⁵, Sam B. Bhayani⁶, Anne Drewry¹, Paul E. Swanson⁷, and Richard S. Hotchkiss^{1,3,8}

¹Department of Anesthesiology, ²Department of Immunology and Pathology, ³Department of Surgery, ⁶Department of Urology, and ⁸Department of Medicine, Washington University School of Medicine, St. Louis, Missouri; ⁴Department of Biomedical Engineering, Washington University, St. Louis, Missouri; ⁵Department of Surgery, St. John's Mercy Medical Center, St. Louis, Missouri; and ⁷Department of Pathology, University of Washington School of Medicine, Seattle, Washington

Rationale: The mechanistic basis for cardiac and renal dysfunction in sepsis is unknown. In particular, the degree and type of cell death is undefined.

Objectives: To evaluate the degree of sepsis-induced cardiomyocyte and renal tubular cell injury and death.

Methods: Light and electron microscopy and immunohistochemical staining for markers of cellular injury and stress, including connexin-43 and kidney-injury-molecule-1 (Kim-1), were used in this study.

Measurements and Main Results: Rapid postmortem cardiac and renal harvest was performed in 44 septic patients. Control hearts were obtained from 12 transplant and 13 brain-dead patients. Control kidneys were obtained from 20 trauma patients and eight patients with cancer. Immunohistochemistry demonstrated low levels of apoptotic cardiomyocytes (<1–2 cells per thousand) in septic and control subjects and revealed redistribution of connexin-43 to lateral membranes in sepsis ($P < 0.020$). Electron microscopy showed hydropic mitochondria only in septic specimens, whereas mitochondrial membrane injury and autophagolysosomes were present equally in control and septic specimens. Control kidneys appeared relatively normal by light microscopy; 3 of 20 specimens showed focal injury in approximately 1% of renal cortical tubules. Conversely, focal acute tubular injury was present in 78% of septic kidneys, occurring in $10.3 \pm 9.5\%$ and $32.3 \pm 17.8\%$ of corticomedullary-junction tubules by conventional light microscopy and Kim-1 immunostains, respectively ($P < 0.01$). Electron microscopy revealed increased tubular injury in sepsis, including hydropic mitochondria and increased autophagosomes.

Conclusions: Cell death is rare in sepsis-induced cardiac dysfunction, but cardiomyocyte injury occurs. Renal tubular injury is common in sepsis but presents focally; most renal tubular cells appear normal. The degree of cell injury and death does not account for severity of sepsis-induced organ dysfunction.

Keywords: sepsis; apoptosis; necrosis; autophagy; kidney

(Received in original form November 5, 2012; accepted in final form December 27, 2012)

* These authors contributed equally to this work.

This work was supported by National Institutes of Health grants GM44118, GM55194, and GM098391. J.P.G. was supported by a Washington University O'Brien Center Pilot and Feasibility grant (P30 DK07933-05).

Author Contributions: Study design: O.T., K.T., J.P.G., E.W., R.E.F., I.R.E., A.D., P.E.S., and R.S.H. Data collection: O.T., K.T., E.W., R.E.F., B.S., S.J., D.L.J., A.S., J.P.G., S.B.B., P.E.S., and R.S.H. Data analysis: O.T., K.T., E.W., R.E.F., D.L.J., A.S., J.P.G., S.B.B., P.E.S., and R.S.H. Data interpretation: O.T., E.W., R.E.F., I.R.E., J.P.G., P.E.S., and R.S.H. Writing: O.T., J.P.G., and P.E.S.

Correspondence and requests for reprints should be addressed to Richard S. Hotchkiss, M.D., Department of Anesthesiology, Washington University School of Medicine, 660 S. Euclid, St. Louis, MO 63110. E-mail: hotch@wustl.edu

This article has an online supplement, which is accessible from this issue's table of contents at www.atsjournals.org

Am J Respir Crit Care Med Vol 187, Iss. 5, pp 509–517, Mar 1, 2013

Copyright © 2013 by the American Thoracic Society

Originally Published in Press as DOI: 10.1164/rccm.201211-1983OC on January 24, 2013

Internet address: www.atsjournals.org

AT A GLANCE COMMENTARY

Scientific Knowledge on the Subject

Sepsis causes profound myocardial depression, and echocardiography frequently reveals severe biventricular dysfunction. Sepsis also induces renal insufficiency in 30 to 60% of patients, up to half of whom require dialysis. The mechanistic basis for cardiac and renal dysfunction occurring in sepsis is controversial.

What This Study Adds to the Field

Our findings show that cell death is rare in sepsis-induced cardiac dysfunction, but sepsis-induced focal mitochondrial injury does occur. Autophagy is not a major mechanism of cardiomyocyte repair or cell death in sepsis. Connexin-43 translocation, which occurred in cardiomyocytes of septic patients, is suggestive of cell injury and is consistent with cardiac dysfunction being secondary to a “junctionopathy,” although this remains to be established. Renal tubular injury is common in sepsis but present focally; renal tubular regeneration possibly driven by mTOR also appears to be occurring. Renal tubular cell death occurs by necrosis and not by apoptosis or autophagy. This suggests that much of the organ injury is potentially reversible and that efforts to control infection and improve host immunity could decrease mortality.

Sepsis causes profound myocardial depression, and echocardiography frequently reveals severe biventricular dysfunction (1–5). Sepsis also induces renal insufficiency in 30 to 60% of patients, up to half of whom require dialysis (6–10). The mechanistic basis for cardiac and renal dysfunction occurring in sepsis is controversial (1, 5, 7, 9, 11–16). The degree to which apoptosis, necrosis, or autophagy contribute to cardiac and renal dysfunction in sepsis is unresolved (2, 3, 16–19).

Although a few well controlled studies have been performed, extensive cell death in hearts or kidneys in patients dying of sepsis has not been described, leading investigators to postulate that cellular “hibernation” or metabolic suppression and not cell death is the basis of sepsis-induced organ failure (11, 13, 14, 16, 18, 20–22). Cardiac dysfunction in sepsis is reversible, and the majority of renal failure patients who survive sepsis recover baseline renal function; these observations are consistent with organ “hibernation” (1, 3, 13, 18). However, evidence for cardiac and kidney cell injury and death in sepsis does exist. Elevations in troponin-I, a marker of cardiomyocyte injury, typically occur in septic patients and correlate with mortality (23). Other studies examining the

mechanistic basis of renal dysfunction in sepsis reported that ischemic tubular necrosis and apoptosis occur (9, 24–28).

Methodologic advances have improved our understanding of cell death, providing tools to better define the basis of organ dysfunction in sepsis (29, 30). In addition to necrosis and apoptosis, autophagic cell death occurs (29, 30). Autophagy is an adaptive response to sublethal stress, allowing cells to recycle damaged organelles and macromolecules. Although controversial, some investigators maintain that unbridled autophagy results in cell death (29–31). Newly characterized markers of cell injury have also contributed to defining pathologic processes that mediate cell injury. Connexin-43, a critical gap junction protein that regulates cell–cell interaction and forms electrical synapses between adjacent myocytes, is involved in cellular stress responses in heart (32–35). Kidney injury molecule 1 (Kim-1), a transmembrane protein expressed in damaged proximal tubular epithelial cells, is a sensitive biomarker of kidney injury (36, 37). Mammalian target of rapamycin (mTOR), a serine/threonine kinase activated during stress, regulates cellular metabolism, proliferation, and survival (38).

This investigation determined the degree to which cell injury and death are responsible for sepsis-induced cardiac and renal dysfunction. Electron microscopy was performed to evaluate subcellular effects of sepsis and to identify autophagic vacuoles. Some of the results of these studies have been previously reported in the form of an abstract (39).

METHODS

Sepsis Inclusion and Exclusion Criteria

Septic patients who died in surgical and medical intensive care units were studied. Most patients were previously included in a recently completed parallel study examining effects of sepsis on immunity (40). Sepsis was defined as microbiologically proven, clinically proven, or suspected infection and presence of systemic inflammatory response syndrome (SIRS) (41). Patients receiving corticosteroids (>300 mg/d of hydrocortisone) or other immunosuppressive medications, patients with chronic viral infections, and patients with autoimmune disease were excluded. Patients with preexisting dialysis-dependent renal failure were excluded from kidney but not heart analysis.

Control Patient Inclusion Criteria

Control tissues for electron microscopy (EM) were obtained from patients undergoing nephrectomy for renal cancer. Tissue remote from tumor site was selected. Control tissue for light microscopy (LM) and immunohistochemistry (IHC) was obtained from paraffin-embedded tissue from critically ill patients, identified by retrospective chart review, who had sustained acute kidney trauma necessitating nephrectomy.

Control hearts were obtained from Mid-America Transplant (St. Louis, MO), comprising organ donors whose hearts were not acceptable for donation because of preexisting conditions or age. Failing hearts were obtained from patients who received heart transplants. Control patient exclusion criteria were identical to sepsis.

Studies were approved by Washington University and St John's Hospital Human Research Protection offices. Further details are provided in the online supplement.

Tissue Harvesting

Tissues were harvested via limited bedside autopsy 30 to 180 minutes postmortem. Midmyocardial left ventricular free wall and renal corticomedullary junction were selected.

Immunohistochemical Detection of Necrotic and Apoptotic Cell Death

In addition to LM evaluation of hematoxylin and eosin (H&E)-stained tissues, sections were examined for apoptosis using antibodies to active caspase-3, cleaved cytokeratin-18, and cleaved poly(ADP-ribose) polymerase (PARP) (40).

Histopathologic Assessment: Kidneys

The number of globally sclerosed glomeruli and the total number glomeruli were recorded. Arterial intimal fibrosis, arteriolar hyalinosis, interstitial fibrosis, and interstitial inflammation were scored according to established criteria (42). Acute tubular injury (ATI) was defined as tubular dilatation, epithelial flattening, cell sloughing, or coagulative necrosis. ATI was quantified in cortex, corticomedullary junction, and medulla by determining the number of injured tubules per 200 total tubules per region. ATI grading was performed in a blinded fashion.

Immunohistochemical Studies

IHC for connexin-43 and Kim-1 was used to detect cardiomyocyte and RTC injury, respectively. IHC for phosphorylated-mTOR (mTOR), an indicator of cell stress, was also performed.

Detection of Renal Tubular Cell Proliferation via Ki-67

Ki-67 staining was performed on a Benchmark Ultra platform (Ventana, Oro Valley, AZ) using prediluted antibody.

Electron Microscopy

A minimum of 8 to 10 random fields were examined at 2,460 to 3,070 \times magnification in blinded fashion (43). In kidney, tubules at the corticomedullary junction were targeted. Higher magnifications (5,000–25,000 \times) were used in abnormal areas to evaluate organelle changes.

Statistical Analysis

Group differences were analyzed by two-tailed, nonparametric *t* test (Mann-Whitney U test) using GraphPad-Prism 5.0. Significance was accepted at $P \leq 0.05$. Data are expressed as mean \pm SD.

RESULTS

Patient Clinical Characteristics

Ventilator-associated pneumonia and peritonitis were the most frequent causes of sepsis (Table 1; see Table E1 in the online supplement). Other causes included necrotizing fasciitis, retroperitoneal abscess, and infected intravascular catheters.

Control hearts from 12 heart transplant recipients and 13 brain-dead organ donors were studied (Table 1; Table E2). Control kidneys from eight renal cancer patients and 20 trauma patients were used for EM and IHC, respectively (Table E3).

Mean ages of septic and control patients were 67 ± 19 and 48 ± 19 years, respectively. Median ICU days for septic patients were 8 (range, 1–195); mean duration of sepsis was 7 days.

Sepsis-induced Cardiac Dysfunction

Troponin-I was quantitated in 30 of 38 septic patients and was elevated in 19 patients (0.47 ± 0.89 ng/ml) (Table E4). Inotropic agents were required in 32 of 38 septic patients. Echocardiography obtained in 21 septic patients demonstrated mean ejection fractions of $54 \pm 15.8\%$ while on inotropic and/or vasopressor support.

Sepsis-induced Renal Dysfunction

A total of 36 of 39 septic patients developed acute kidney injury defined by AKIN criteria; 14 of 36 required dialysis (Table E5) (8).

Cardiac Microscopic and Immunohistochemical Findings

Septic and control hearts exhibited LM evidence of chronic disease, including varying degrees of interstitial fibrosis and cardiomyocyte hypertrophy (Figures 1A and 1B; see Figure E1 in the online supplement). Cytoplasmic vacuolization associated with presumed reversible hypoxic injury (myocytolysis)

TABLE 1. CLINICAL CHARACTERISTICS OF PATIENTS

| | Patients with Sepsis | Control Patients | |
|----------------------------------|----------------------|------------------|------------|
| | | Heart | Kidney |
| Age, mean (range) | 67 (18–94) | 56 (26–76) | 41 (18–85) |
| Sex, M/F | 24/20 | 16/9 | 22/7 |
| Sites of infection | | | |
| Intrapelvic abscess | 4 | | |
| Intravascular catheters | 3 | | |
| Necrotizing fasciitis | 2 | | |
| Osteomyelitis | 1 | | |
| Pneumonia | 27 | | |
| Peritonitis | 19 | | |
| Retroperitoneal abscess | 1 | | |
| Urinary tract infection | 2 | | |
| Pathology | | | |
| Heart transplant recipients | | 12 | |
| Neurologic death | | 13 | |
| Trauma | | | 20 |
| Cancer | | | 9 |
| Days in hospital, median (range) | 11 (1–195) | | |
| Days in ICU, median (range) | 8 (1–195) | | |
| Days of sepsis, median (range) | 4 (1–40) | | |
| Comorbidities | | | |
| Diabetes | 12 | | |
| Heart disease | 30 | | |
| Morbid obesity | 5 | | |
| Neurologic | 6 | | |
| Renal disease | 3 | | |
| Respiratory | 9 | | |
| Organ failure | | | |
| Circulatory (vasopressors) | 39 | | |
| Hepatic | 13 | | |
| Renal | 30 | | |
| Respiratory | 37 | | |
| Microbiology | | | |
| Gram positive | 21 | | |
| Gram negative | 28 | | |
| Fungal | 3 | | |

was more common in control subjects ($P < 0.01$) (Figure E1), but acute myocardial necrosis was uncommon. Differences in cardiac fibrosis and myocytolysis also existed between control failing hearts obtained from transplant recipients and control hearts from brain-dead organ donors (Figure E2). No apoptotic cardiomyocytes were seen in any specimen by LM.

Examination of cardiomyocyte apoptosis via immunohistochemical staining (i.e., expression of cleaved PARP, active caspase-3, and cytokeratin-18) demonstrated rare cardiomyocyte apoptosis in septic and control cells ($<0.2\%$ cells; Figure E3), which were not different.

Expression of connexin-43 was demonstrated in all cases. Distribution of reactivity along intercalated discs was variable within and between samples in both groups, whereas expression along lateral cell membranes was detected only in septic hearts (7/38 septic vs. 0/23 control; $P < 0.02$) (Figures 1C and 1D; Figure E1).

EM Studies: Heart

EM was performed on 17 septic hearts and in seven control hearts. Although overall architecture was generally well preserved, loss of register of the contractile apparatus or compression of the Z-band interval (“contraction-banding”) was noted in similar percentages of both groups (septic, 5/17; control, 2/7; Figure E4). Hydropic mitochondria (compatible with a mitochondrial injury score of ≥ 3) (44) were present in six septic patients but in no control subjects ($P < 0.05$); structural changes to mitochondrial cristae (vacuoles and collapse) occurred in similar numbers in both groups (Figure 1; Figure E4). The former change was inconsistently associated with longitudinal separation

(splaying) of contractile fibers. Autophagosomes were uncommon in most samples (Figure 1H).

Kidney Light Microscopic and Apoptosis Examination

LM of control kidneys showed normal-appearing glomeruli and tubules with few inflammatory cells (Table E7). Focal ATI involving approximately 1% of proximal renal tubular cells occurred in 3 of 20 (15%) control kidneys. Focal coagulative-type tubular necrosis involving less than 5% of renal tubular cells occurred in 2 of 20 (10%) control kidneys.

Septic kidneys had increased global glomerulosclerosis, arteriolar hyalinosis, and arterial intimal fibrosis compared with control kidneys (Figure 2; Table E7). Although the majority of microscopic fields appeared normal, focal ATI was common and occurred in 30 of 39 (77%) septic patients, affecting $10.3 \pm 9.5\%$ corticomedullary junction tubules and $5.9 \pm 9.8\%$ cortical tubules. Medullary tubular epithelial cell sloughing occurred in 35 of 36 (97%) patients, affecting $18.7 \pm 11.7\%$ of tubules. Focal coagulative-type tubular necrosis occurred in 17 of 39 (44%) patients, typically involving less than 5% of renal tubular cells. Microvascular glomerular thrombosis, renal cortical infarction, and renal abscess occurred in one septic patient each.

Additional discriminating findings in sepsis were isometric proximal tubular vacuolization, which occurred in 30 of 39 (77%) septic patients versus 3 of 20 (15%) control subjects ($P < 0.001$), and calcium phosphate crystals, which were present in 19 of 39 (49%) septic patients versus 1/20 (5%) control subjects ($P < 0.001$) (Figure E5).

Renal tubular cell apoptosis was rare, occurring in less than approximately 0.3% of cells by all three detection methods (Figure E6). Renal tubular cell apoptosis was increased in sepsis when quantitated by cytokeratin-18 but not by active caspase-3 or cleaved PARP ($P < 0.001$).

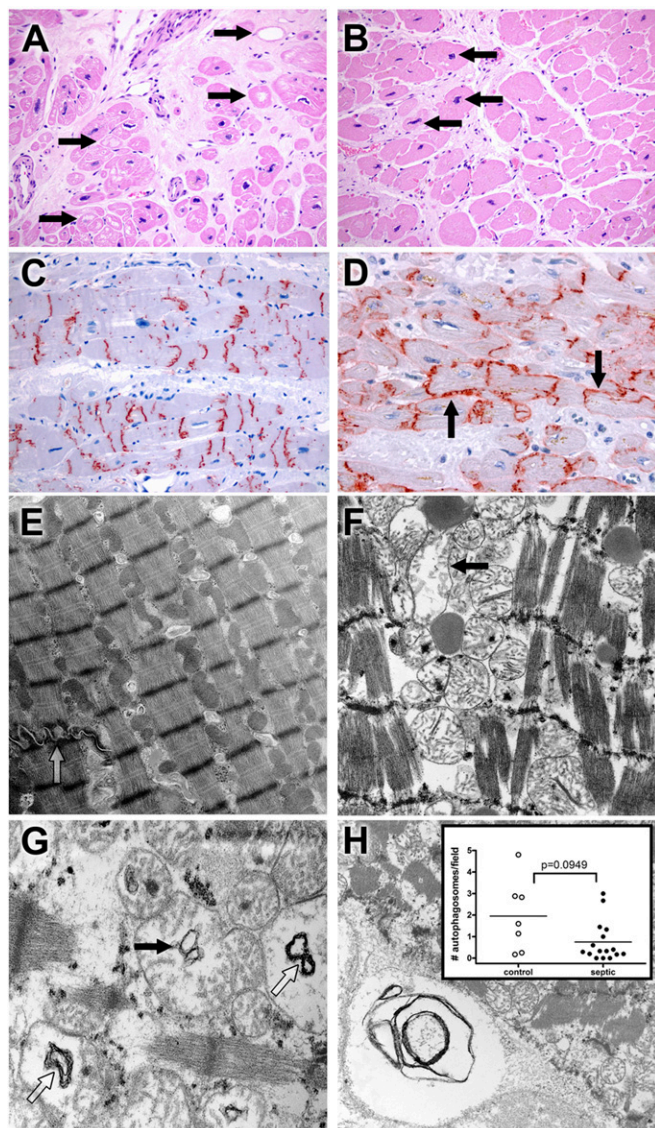
Kim-1 and Phospho-mTOR Immunostaining

In control kidneys, Kim-1 was positive in $1.3 \pm 2.9\%$ and $0.8 \pm 2.7\%$ of corticomedullary junction and cortical labyrinth tubules, respectively (Figure 2; Table E8). Kim-1 expression was markedly increased in septic kidneys (i.e., $32.3 \pm 17.8\%$ and $19.6 \pm 16.9\%$ in corticomedullary junction and cortical labyrinth tubules, respectively [$P < 0.001$]) (Figure 2H). Kim-1 corticomedullary junction tubular expression was also higher in hemodialysis-dependent septic patients versus non-hemodialysis-dependent septic patients ($44.4 \pm 16.0\%$ vs. $25.4 \pm 14.9\%$, respectively; $P < 0.01$). Kim-1 positivity limited to apical membranes typified injured renal tubular cells, accompanied with loss of height and brush border (Figure 2F; Figure E7). Predominantly cytoplasmic Kim-1 reactivity typified severely flattened renal tubular cells (Figure 2).

mTOR was positive in $20.5 \pm 11.5\%$ versus $35.6 \pm 14.7\%$ corticomedullary junction tubules in control and septic kidneys, respectively ($P < 0.01$) (Figure 3). mTOR-positive cells exhibited two distinct morphologic patterns. Similar to Kim-1, mTOR was positive in damaged renal tubular cells that appeared flattened (Figure 3B; Figure E8). Kim-1 and mTOR stains on serial sections of injured renal tubular cells with this pattern showed colocalization of these markers (Figure E9). Far less commonly, mTOR positivity occurred in injured renal tubular cells with isometric vacuolization; these cells did not typically coexpress Kim-1.

EM Studies: Kidney

EM was performed on 14 septic and 9 control kidneys. Isometric vacuolization in septic proximal tubules was associated with hydropic



mitochondria (six cases) or marked dilation of membrane-bound vacuoles of presumed lysosomal derivation (six cases) with or without autophagocytosis (Figure 4; Figures E10 and E11; Table E6). No case contained both. Two septic cases lacked these changes in LM and EM. Only one control sample had hydropic mitochondria, and none contained enlarged lysosomes. The difference between groups was significant ($P = 0.003$). In sepsis, proximal tubular epithelial cells showed varying degrees of apical membrane injury, including loss of ciliated brush border. The latter was seen in cuboidal cells (often in clusters) with intact apical membranes, suggestive of regeneration and repair, or in columnar cells devoid of apical membranes, with loss of apical cytoplasm into the lumen. In the latter, organelles in extruded cytoplasm were often in autophagocytic vacuoles, whereas basal cytoplasm was intact (Figure 4; Figures E10 and E11). Less commonly, entire damaged cells were necrotic and detached from basal lamina, occasionally appearing downstream in otherwise intact tubules (Figure E11B). Necrotic cells and cell debris were significantly less common in control kidneys ($P = 0.02$). Mitochondrial membrane damage (as also seen in cardiomyocytes) and dilation of endoplasmic reticulum were seen in septic kidneys; only the former was noted (and much less commonly) in control kidneys. Autophagosomes were more common in septic

Figure 1. Light microscopy and ultrastructural findings in heart. (A) Myocytolysis is common in control cardiac myocytes. Hearts were obtained from septic or control patients. Control hearts were failing hearts from patients undergoing heart transplantation or hearts from brain-dead organ donors whose hearts were not acceptable for transplantation (see METHODS). Although most myocardial cells were unremarkable in most histologic fields in control and septic samples, large, pale vacuoles in subendocardial myocytes (myocytolysis; arrows), a putative feature of reversible hypoxic injury, were more common in control samples ($P < 0.01$) (Figure E1). Note also expansion of interstitial fibrous tissue and enlargement of myocyte nuclei (hypertrophy). Original magnification: $\times 200$. (B) Myocyte hypertrophy is common in septic cardiac samples. Although not specific for sepsis, many septic hearts exhibited conspicuous enlargement of myocyte nuclei (hypertrophy; arrows), often in a setting in interstitial fibrosis. Original magnification: $\times 200$. (C) Connexin-43 is present on intercalated discs in control hearts. Strong granular staining of the intercalated discs is seen in this example. Punctate staining of cytoplasm away from the intercalated discs most likely represents intracellular microtubule-mediated transport. Original magnification: $\times 200$. (D) Connexin-43 localizes to lateral cell membranes in some septic specimens. In addition to labeling the intercalated discs, antibodies to connexin-43 also reveal reactivity along lateral myocyte membranes (arrows) in a subset of septic samples. Lateralization of connexin-43 was more common in septic patients ($P < 0.05$) (Fig. E1). Original magnification: $\times 400$. (E) Electron microscopy of control cardiac muscle. Contractile elements, with distinct Z-bands, are aligned in register. Mitochondria and other organelles occupy space between myofilaments and contractile fibers; most appear normal. Elements of sarcomplasmic reticulum (T tubules) are also evident. A portion of a normal-appearing intercalated disc is present (open arrow). Isolated lipid droplets are present. Original magnification: $\times 9,730$. (F) Electron microscopy of septic cardiac muscle. Contractile elements are in register but are mildly splayed in areas. Mitochondria are relatively normal in appearance but with focal hydropic change (arrow); crista are generally intact. Lipid is present. Original magnification: $\times 12,800$. (G) Mitochondrial abnormalities in sepsis. Hydropic change (edema of the mitochondrial matrix) is associated with cystic alterations of the crista (closed arrow) and collapse into small myelin-like clusters (open arrow). Original magnification: $\times 18,400$. (H) Autophagy in cardiac muscle. Organelle-derived membrane products are packaged in an autophagosome (lower left corner). Original magnification: $\times 9,730$. Insert: Dot plot of average autophagosomes per 3,070 \times image. The range is wider among control samples, with a higher mean compared with septic samples, but these findings did not reach statistical significance.

kidneys (i.e., 4.61 ± 3.82 vs. 1.54 ± 0.75 per high-powered field [original magnification: $\times 3,070$] for septic and control, respectively; $P = 0.011$); however, there was no evidence of autophagic cell death. No epithelial apoptosis was noted in any sample. Basolateral and nuclear membranes were well preserved, arguing against preservation-related changes (autolysis).

Renal Tubular Cell Proliferation via Ki-67 Immunostaining

The percentage of renal tubular cells in the corticomedullary junction positive for Ki-67 was increased almost 3-fold in septic versus control kidneys (i.e., 0.99 ± 1.05 vs. 0.34 ± 0.47 , respectively [$P < 0.005$]) (Figure E12).

DISCUSSION

Myocardial depression and renal failure are hallmarks of sepsis, but the mechanistic basis for sepsis-induced organ dysfunction is controversial (1–5). The present study represents the first comprehensive examination of cell death and organelle injury in patients with sepsis-induced cardiac and renal failure. The vast majority of septic patients (32 of 38) were in shock, requiring the use of inotropic agents and/or vasopressors to maintain adequate mean arterial pressure and/or oxygen delivery (Table E4). Shock in patients with sepsis could be due to primary myocardial

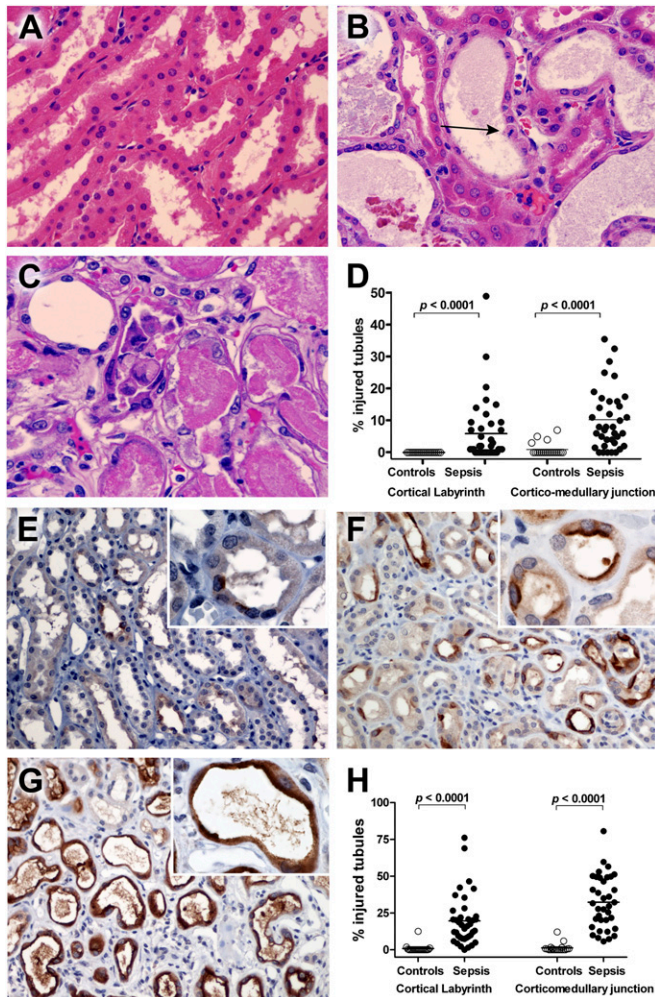


Figure 2. Hematoxylin and eosin (H&E) and kidney injury molecule 1 (Kim-1) immunostaining in kidney. (A) Corticomedullary junction from a control kidney. Note the normal-appearing renal tubular cells with minimum tubular debris. H&E staining. Original magnification: $\times 600$. (B) Corticomedullary junction from a septic kidney demonstrating tubular dilation with epithelial flattening. A mitotic figure is present (arrow), indicating regenerative change. H&E staining. Original magnification: $\times 600$. (C) Corticomedullary junction from a different septic kidney demonstrating proximal tubular coagulative necrosis with epithelial cell sloughing. H&E staining. Original magnification: $\times 600$. (D) Acute tubular injury, defined as tubular dilatation, epithelial flattening, cell sloughing, or coagulative necrosis, was graded by light microscopy in blinded fashion. Acute tubular injury was quantified in cortical labyrinth and corticomedullary junction by counting number of injured tubules per 200 total tubules per region. There was a statistically significant increase in acute tubular injury in septic kidneys compared with control kidneys. Although both the cortical labyrinth and corticomedullary junction showed increased injury, there was more extensive damage in the corticomedullary junction. (E) Kim-1 immunoreactivity of corticomedullary junction from a control kidney. Kim-1 staining is focally present in a limited number of the tubules and tubular epithelial cells. Kim-1 immunostaining. Original magnification: $\times 200$ and $\times 1,000$ (insert). (F) Kim-1 immunoreactivity is markedly increased in corticomedullary junction tubules from a septic kidney. Kim-1 expression is primarily localized on apical surface of the tubular epithelial cells with loss of height and brush borders. Original magnification: $\times 200$ and $\times 1,000$ (insert). (G) Kim-1 immunoreactivity of corticomedullary junction from a septic kidney. The cytoplasmic staining of Kim-1 is present on flattened tubular epithelial cells in dilated tubules. Original magnification: $\times 200$ and $\times 1,000$ (insert). (H) Acute tubular injury quantitated by Kim-1 immunoreactivity. Kim-1 staining slides were evaluated in a blinded fashion and scored (in percentage) in two different areas (cortical labyrinth and corticomedullary junction). Data are graphed as percentage injured tubules for Kim-1 staining in both areas. Each data marker represents an individual patient. Horizontal lines represent mean values. Kim-1 expression in septic kidneys is significantly higher than that of control kidneys in both areas.

depression, sepsis-induced vascular failure (vasoplegia), or a combination of both. Therefore, it is difficult to know the extent of sepsis-induced myocardial depression without comparing current echocardiographic data with premorbid echocardiographic information. This information is available for a subset of septic patients (Table E4). Some patients who developed sepsis had similar or unchanged high normal ejection fractions. Conversely, other patients had slightly improved ejection fractions during sepsis or marked decreases in ejection fraction during sepsis. There are several complicating factors in determining the extent of sepsis-induced myocardial depression in these patients. Sepsis-induced vasoplegia results in decreased afterload, which can result in improved ejection fraction. Second, many patients were on inotropic agents and/or vasopressors, which can increase myocardial contractility. In this regard, 13 of the 38 septic patients were on dobutamine or epinephrine, inotropic agents that can markedly increase contractility and ejection fraction. Finally, sepsis-induced myocardial depression tends to be most severe during the most fulminant stage of the disease, and cardiac function tends to improve as the sepsis becomes less severe. It is not always possible to obtain echocardiography during the most profound stages of sepsis; therefore, the present results may not reflect the most severe depression. Despite these limitations, many patients had low ejection fractions while on potent inotropic agents, and the ejection fraction of 54% in the present study is consistent with other studies of septic patients who were on vasoactive agents (45).

Light microscopy of septic hearts did not reveal evidence of irreversible acute injury or cell death. However, modest increases

in troponin-I occurring in selected septic patients is consistent with cardiomyocyte injury. EM demonstrated focal cardiomyocyte mitochondrial membrane injury in control subjects and in septic patients. Translocation of connexin-43 to the lateral cardiomyocyte membrane was detected only in septic patients and only in a subset of these patients. Lateralization of connexin-43 is additional evidence of myocyte injury (32–35). Thus, sepsis does not induce significant cardiomyocyte cell death but does induce changes consistent with mitochondrial injury and cardiomyocyte uncoupling. State-of-the-art *in vivo* ^{31}P NMR spectroscopy showed that sepsis-induced myocardial depression is not due to bioenergetic failure (15). This suggests that mitochondrial injury is limited in scope or is insufficient to impair function.

With these observations in mind, two key questions remain: What is the mechanistic basis of myocardial depression in sepsis, and is it beneficial or detrimental? Studies examining the basis of depressed myocardial contractility in sepsis showed that $\text{TNF-}\alpha$ and $\text{IL-1}\beta$ impair cardiac and cardiomyocyte contractility (46–48). These cytokines also induce mitochondrial injury (44). Although a direct relationship between morphologic changes in mitochondria and cardiomyocyte depression cannot be proven, the possible effect of mitochondrial swelling on metabolic activity of the septic cardiomyocyte is relevant to potential explanations for sepsis-induced myocardial depression, including a “hibernation” response and myocardial “stunning.” The latter is a well recognized phenomenon occurring after myocardial ischemia and may represent a response that is analogous to the myocardial “hibernation” that is postulated to occur in sepsis (13, 14, 18, 49). Abnormalities in calcium homeostasis and defects in cardiomyocyte

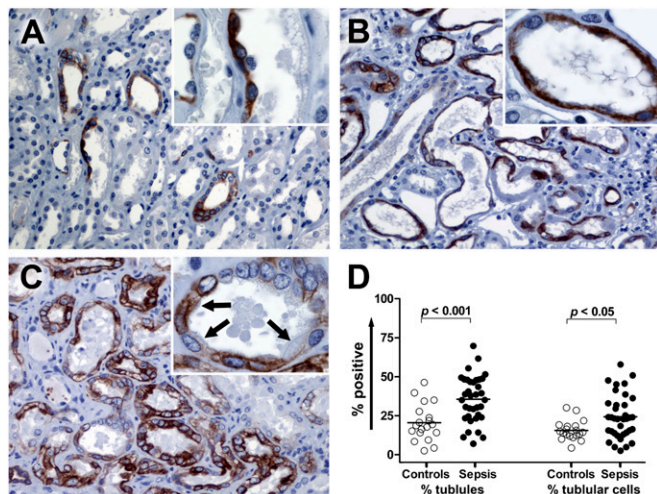


Figure 3. Phospho-mTOR (mTOR) immunostaining in kidney. (A) Corticomedullary junction from a control kidney. Focal mTOR staining is present in proximal tubules with flattened epithelium and collecting tubules. The mTOR-positive proximal tubule demonstrates slightly enhanced nuclear prominence (*insert*). Original magnification: $\times 200$ and $\times 1,000$ (*insert*). (B) Corticomedullary junction from a septic kidney demonstrating the mTOR expression on dilated tubules with flattened epithelial cells. Original magnification: $\times 200$ and $\times 1,000$ (*insert*). (C) Corticomedullary junction from a septic kidney. Strong mTOR expression is present in multiple renal tubular cells. In some renal tubular cells that are mTOR positive, fine brush borders remain (*insert, arrows*). Original magnification: $\times 200$ and $\times 1,000$ (*insert*). (D) Comparison of mTOR expression in corticomedullary junction tubules. mTOR expression was evaluated in a blinded fashion and scored. Data are presented in two ways: percentage of mTOR-positive tubules and percentage of mTOR-positive tubular cells. Each data marker represents an individual patient. Horizontal lines represent mean values. mTOR expression in septic kidneys is significantly higher than control kidneys for tubules and tubular cells.

coupling due to abnormal cardiac gap junctions have also been proposed as potential causes of sepsis-induced cardiac depression (11, 50). Although sepsis-induced myocardial suppression is occasionally lethal, moderate sepsis-induced “hibernation” could be advantageous by preventing stress-induced cardiac injury (1, 18, 49).

Previously, we reported that sepsis-induced renal failure was notable for a lack of extensive cell death (51). The present study, using more sensitive detection methods, confirmed a lack of diffuse renal tubular cell death but did reveal tubular injury. Damaged renal tubular cells were significantly more numerous in sepsis, a finding corroborated by EM, where one reproducible abnormality was mitochondrial swelling. Although renal tubular cell injury occurred in sepsis, the majority of renal tubules in most septic patients appeared normal by light microscopy. EM and Kim-1 immunostaining are more sensitive indicators of cell injury and highlighted more extensive yet subtle damage (36, 37). The subcellular nature of the observed renal tubular cell injury is unlikely to be the sole explanation for the magnitude of the loss of renal function suffered by many septic patients (14 patients in our septic cohort required hemodialysis). Rigorously controlled animal models have also failed to reveal widespread cell death in sepsis despite significant renal dysfunction (7, 9, 15, 16, 21, 24, 52). Investigators have struggled to mechanistically define the basis of sepsis-induced renal failure (7, 9, 16, 24, 26). Proposed explanations include immune-mediated injury, apoptosis or necrosis of renal tubular cells, and metabolic “hibernation.” Most septic patients who survive severe renal dysfunction eventually

return to baseline renal function. Unlike heart, however, recovery of renal function can be prolonged, and patients are more prone to chronic renal disease (8). Our findings agree with work by other investigators who report that in certain types of acute renal failure including sepsis, most renal tubular cells are healthy or reversibly injured (7, 10, 26). Our findings do not agree with investigators who have postulated that apoptosis is a major mechanism of sepsis-induced kidney injury (25).

In addition to injured renal tubular cells, light and electron microscopy demonstrated cells with morphologic features of tubular regeneration, including epithelial simplification with nuclear enlargement and clustering (53). Many of these cells were phospho-mTOR positive (Figures 3C and 4G). mTOR has diverse actions, including cell differentiation and proliferation, thereby supporting the concept that tubular cell regeneration and proliferation is an important element of renal recovery in acute kidney injury (7). Ki67 immunostaining confirmed that renal tubular cell proliferation was increased in septic versus control cells (Figure E12).

Septic kidneys also exhibited increased renal tubular cell vacuoles, previously described in sepsis (52) and in foci of intraluminal calcium phosphate crystals. Vacuoles appeared coarse or finely dispersed. Coarse-appearing vacuoles correlated with the presence of swollen, injured mitochondria by EM, whereas fine vacuoles correlated with presence of swollen lysosomes. Mitochondrial injury has been proposed as a significant mechanism of septic renal dysfunction in animal models (52). Calcium phosphate crystals, which occurred in approximately 50% of septic patients, also occur in tumor-lysis syndrome and induce renal tubular cell injury.

A final observation that was prominent in septic kidneys was the shedding of apical cytoplasm and renal tubular cells (necrotic or grossly viable) into tubular lumens (Figure 4; Figure E12). TNF- α and IL-1 α induce similar renal tubular cell shedding, thus providing a potential mechanistic link of cardiac and renal injury (52, 54).

It is informative to compare the present study with a previous postmortem study from our group conducted over a decade ago (51). The present study demonstrates much more evidence of cell injury in heart and kidney during sepsis than previously appreciated. Using extensive EM, the present study shows focal mitochondrial injury in hearts and kidneys in a subset of septic patients. The increase in cardiomyocyte connexin-43 positivity in sepsis is supportive evidence of cardiac injury. EM also demonstrated that autophagy, which was not widely recognized as a major cellular stress response until relatively recently, was significantly up-regulated in septic kidneys. There was no evidence of unbridled renal tubular cell autophagy as a mechanism of cell death. Focal renal tubular cell injury and necrosis are much more common than previously appreciated, a finding confirmed by conventional light microscopy, Kim-1 immunostaining, and EM. An additional potential new mechanism of renal injury identified in the present study is the high incidence of calcium phosphate crystals in sepsis. The increase in renal tubular cell Ki67 positivity in sepsis indicates that cell proliferation, possibly driven by mTOR, may be a major restorative response to renal injury.

The present results showing a paucity of cell death in hearts and kidneys of patients dying of sepsis raises the question: Why do patients with sepsis die? Postmortem studies of septic patients demonstrated most cell death occurring in immune and gastrointestinal epithelial cells and, to a lesser extent, in hepatocytes (51, 55). These findings fail to explain mortality in sepsis. A recent postmortem study of 235 ICU patients admitted with sepsis revealed that at autopsy approximately 80% of patients had unresolved infections (56). These studies, together with the present work, indicate that organ recovery is possible even late in sepsis and that better survival may occur with improved control of infections or enhanced host immunity (57).

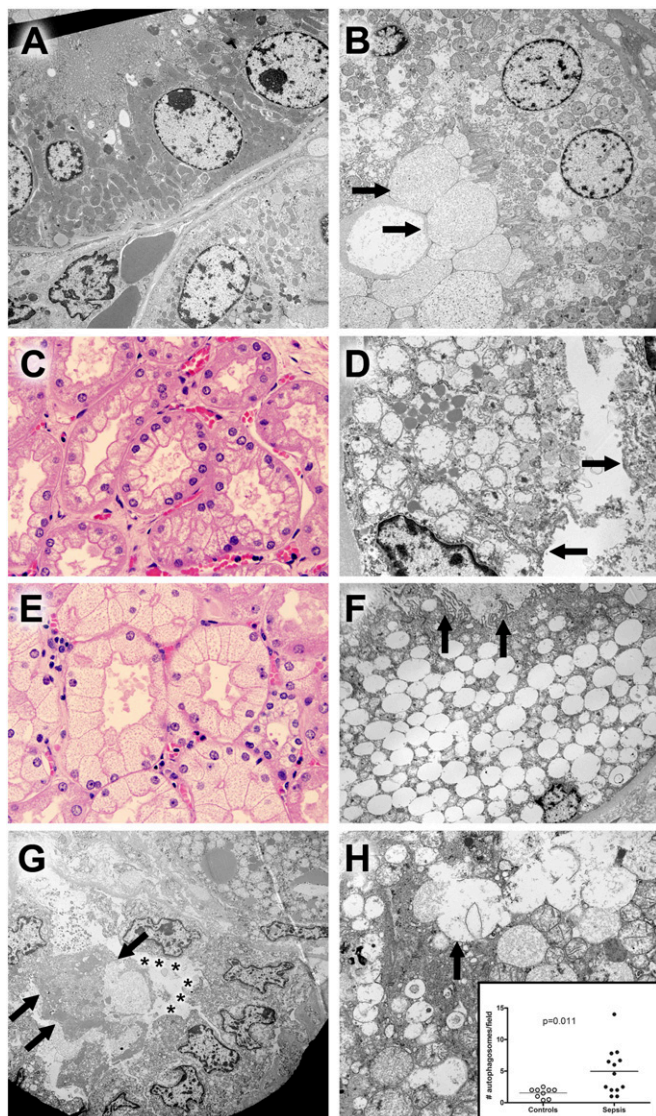


Figure 4. Hematoxylin and eosin (H&E) and electron microscopic findings in kidney. (A) Ultrastructure of normal tubules from a control sample. A proximal tubule is shown in the upper half of this image. Cells are low columnar with uniform round nuclei. The apical membrane (*upper left*) comprises uniform microvilli that project into the lumen (not shown). Mitochondria are large, with relatively dark profiles. Few lysosomes are seen. In the lower half of the image, cells with fewer and smaller mitochondria are present. No microvillus brush border is present. These are distal tubular epithelial cells. Original magnification: $\times 3,070$. (B) Proximal tubule epithelial damage in sepsis. In contrast to normal proximal tubular epithelium, the cytoplasm of these cells contains scattered dilated lysosomes, some with complex internal membrane structure, consistent with autophagy. Although the microvillus brush border is focally present, it is clear that this and other elements of apical membranes have been lost on some cells; in these areas, dilated organelles and cytoplasmic appear to be extruded into the lumen in a manner analogous to apocrine secretion, resulting in accumulation of membrane-bound cell debris (*arrows in lower left hand corner*). Original magnification: $\times 2,460$. (C) Corticomedullary junction from a septic patient demonstrating coarse vacuolization of the proximal tubules. H&E staining. Original magnification: $\times 600$. The corresponding electron microscopic image from this kidney is seen in adjacent view (4D). (D) Hydropic mitochondria in cells with coarse vacuolization. In this proximal tubule, epithelial cells contain enlarged, hydropic mitochondria with damaged crista. Apical membranes are damaged, with loss of the microvillus brush border (*arrows*). Lipid droplets are conspicuous. Original magnification: $\times 6,150$. (E) Corticomedullary junction from a different septic patient showing isometric fine vacuolization of the proximal tubules. H&E staining. Original magnification: $\times 600$. The corresponding electron microscopic image from this kidney is seen in an adjacent view (4F). (F) Dilated lysosomes in cells from septic kidney with isometric fine vacuolization. In this proximal tubule, epithelial cells are expanded by enlarged, focally fused membrane-bound structures. Absent obvious autophagic characteristics or evidence of mitochondrial breakdown, these are best interpreted as lysosomes. Relatively normal mitochondria and other cytoplasmic elements (as well as the nucleus) are displaced to the periphery of the cell. Apical membranes still retain some (but not all) microvilli (*arrows*), and cell debris (focally with features of autophagosomes) occupies the tubule lumen. Original magnification: $\times 2,460$. (G) Damage and regeneration in proximal tubules. In the upper right hand corner of the image, a cell with hydropic mitochondria and large lipid droplets is present. In the lower half of the image, a proximal tubule with three important features is highlighted: 1) detachment and sloughing of a cell into the lumen (*arrows*) and 2) loss of the microvillus brush border (*asterisks*) in a series of cuboidal epithelial cells that also exhibit 3) clustering of nuclei. The latter feature has been suggested as a morphologic corollary of regenerating tubular epithelial cells. Original magnification: $\times 1,840$. (H) Autophagy in septic tubular epithelium. In this image, relatively normal mitochondria are juxtaposed with dilated lysosomal structures, some of which (*arrow*) are fused with adjacent structures or contain membrane fragments (autophagosomes). Mitochondrial membrane damage is also apparent. Original magnification: $\times 6,150$. *Insert:* Dot plot of average autophagosomes per $3,070\times$ field in septic and control samples. Although nearly all samples had recognizable autophagic elements, the mean number per image was significantly increased in septic kidneys. Each *dot* represents an individual patient.

In conclusion, cell death is rare in sepsis-induced cardiac dysfunction, but sepsis-induced focal mitochondrial injury does occur. Autophagy is not a major mechanism of cardiomyocyte repair or cell death in sepsis. Connexin-43 translocation, which

occurred in cardiomyocytes of septic patients, is suggestive of cell injury and is consistent with cardiac dysfunction being secondary to a “junctionopathy,” although this remains to be established. Renal tubular injury is common in sepsis but presents focally; renal tubular regeneration possibly driven by mTOR also appears to be occurring. Renal tubular cell death occurs by necrosis and not by apoptosis or autophagy. Calcium phosphate crystals occur in renal tubules in approximately 50% of patients and may be contributing to renal failure. Although in some septic patients the degree of renal tubular injury was sufficient to explain renal failure, in most septic patients the majority of renal tubular cells appeared normal by light microscopy. Thus, the degree of cell injury and death may not account for the severity of renal failure in all patients with sepsis. This suggests that much of the organ injury is potentially reversible and that efforts to control infection and improve host immunity could decrease mortality.

Author disclosures are available with the text of this article at www.atsjournals.org.

Acknowledgment: The authors thank the nurses and staff of the surgical and medical intensive care units at Barnes Jewish Hospital and St John's Hospital and the Mid-America Transplant, St. Louis, MO, and Akshar Patel and Dr. Kathryn A. Yamada of the Translational Cardiovascular Biobank & Repository at Washington University, supported by NIH/CTSA grant UL1 TR000448 and funds from the Richard J. Wilkinson Trust, for their help.

References

- Parrillo JE. Pathogenetic mechanisms of septic shock. *N Engl J Med* 1993;328:1471–1477.
- Zanotti-Cavazzoni SL, Hollenberg SM. Cardiac dysfunction in severe sepsis and septic shock. *Curr Opin Crit Care* 2009;15:392–397.
- Ward PA. The sepsis seesaw: seeking a heart salve. *Nat Med* 2009;15:497–498.
- Hunter JD, Dodd M. Sepsis and the heart. *Br J Anaesth* 2010;104:3–11.
- Kumar A, Haery C, Parrillo JE. Myocardial dysfunction in septic shock. *Crit Care Clin* 2000;16:251–287.
- Schrier RW, Wang W. Acute renal failure and sepsis. *N Engl J Med* 2004;351:159–169.
- Wen X, Murugan R, Peng Z, Kellum JA. Pathophysiology of acute kidney injury: a new perspective. *Contrib Nephrol* 2010;165:39–45.
- Murugan R, Kellum JA. Acute kidney injury: what's the prognosis? *Nat Rev Nephrol* 2011;7:209–217.
- Ishikawa K, May CN, Gobe G, Langenberg C, Bellomo R. Pathophysiology of septic acute kidney injury: a different view of tubular injury. *Contrib Nephrol* 2010;165:18–27.
- Abuelo JG. Normotensive ischemic acute renal failure. *N Engl J Med* 2007;357:797–805.
- Fernandes CJ Jr, Campos AH. Sepsis-induced myocardial depression and calcium mishandling: an acceptable unifying theory? *Crit Care Med* 2008;36:2695–2696.
- Hotchkiss RS, Karl IE. Reevaluation of the role of cellular hypoxia and bioenergetic failure in sepsis. *JAMA* 1992;267:1503–1510.
- Fink MP, Evans TW. Mechanisms of organ dysfunction in critical illness: report from a round table conference held in brussels. *Intensive Care Med* 2002;28:369–375.
- Rudiger A, Singer M. Mechanisms of sepsis-induced cardiac dysfunction. *Crit Care Med* 2007;35:1599–1608.
- Solomon MA, Correa R, Alexander HR, Koev LA, Cobb JP, Kim DK, Roberts WC, Quezado ZM, Scholz TD, Cunnion RE, et al. Myocardial energy metabolism and morphology in a canine model of sepsis. *Am J Physiol* 1994;266:H757–H768.
- Wan L, Bagshaw SM, Langenberg C, Saotome T, May C, Bellomo R. Pathophysiology of septic acute kidney injury: what do we really know? *Crit Care Med* 2008;36:S198–S203.
- Exline MC, Crouser ED. Mitochondrial dysfunction during sepsis: still more questions than answers. *Crit Care Med* 2011;39:1216–1217.
- Abraham E, Singer M. Mechanisms of sepsis-induced organ dysfunction. *Crit Care Med* 2007;35:2408–2416.
- Rosen S, Heyman SN. Difficulties in understanding human “acute tubular necrosis”: limited data and flawed animal models. *Kidney Int* 2001;60:1220–1224.
- Hotchkiss RS, Karl IE. The pathophysiology and treatment of sepsis. *N Engl J Med* 2003;348:138–150.
- Kumar A, Wood K, Parrillo JE. Circulating substances and energy metabolism in septic shock. *Crit Care Med* 2003;31:632–633.
- dos Santos CC, Gattas DJ, Tsoporis JN, Smeding L, Kabir G, Masoom H, Akram A, Plotz F, Slutsky AS, Husain M, et al. Sepsis-induced myocardial depression is associated with transcriptional changes in energy metabolism and contractile related genes: a physiological and gene expression-based approach. *Crit Care Med* 2010;38:894–902.
- John J, Woodward DB, Wang Y, Yan SB, Fisher D, Kinasewitz GT, Heiselman D. Troponin-i as a prognosticator of mortality in severe sepsis patients. *J Crit Care* 2010;25:270–275.
- Jacobs R, Honore PM, Joannes-Boyau O, Boer W, De Regt J, De Waele E, Collin V, Spapen HD. Septic acute kidney injury: the culprit is inflammatory apoptosis rather than ischemic necrosis. *Blood Purif* 2011;32:262–265.
- Lerolle N, Nochy D, Guerot E, Bruneval P, Fagon JY, Diehl JL, Hill G. Histopathology of septic shock induced acute kidney injury: apoptosis and leukocytic infiltration. *Intensive Care Med* 2010;36:471–478.
- Langenberg C, Bagshaw SM, May CN, Bellomo R. The histopathology of septic acute kidney injury: a systematic review. *Crit Care* 2008;12:R38.
- Dunnill MS, Jerrome DW. Renal tubular necrosis due to shock: light and electron-microscope observations. *J Pathol* 1976;118:109–112.
- Mustonen J, Pasternack A, Helin H, Pystynen S, Tuominen T. Renal biopsy in acute renal failure. *Am J Nephrol* 1984;4:27–31.
- Galluzzi L, Maiuri MC, Vitale I, Zischka H, Castedo M, Zitvogel L, Kroemer G. Cell death modalities: classification and pathophysiological implications. *Cell Death Differ* 2007;14:1237–1243.
- Klionsky DJ. Autophagy: from phenomenology to molecular understanding in less than a decade. *Nat Rev Mol Cell Biol* 2007;8:931–937.
- Hotchkiss RS, Strasser A, McDunn JE, Swanson PE. Cell death. *N Engl J Med* 2009;361:1570–1583.
- Beardslee MA, Laing JG, Beyer EC, Saffitz JE. Rapid turnover of connexin43 in the adult rat heart. *Circ Res* 1998;83:629–635.
- Jain SK, Schuessler RB, Saffitz JE. Mechanisms of delayed electrical uncoupling induced by ischemic preconditioning. *Circ Res* 2003;92:1138–1144.
- Chew SS, Johnson CS, Green CR, Danesh-Meyer HV. Role of connexin43 in central nervous system injury. *Exp Neurol* 2010;225:250–261.
- Glukhov AV, Fedorov VV, Kalish PW, Ravikumar VK, Lou Q, Janks D, Schuessler RB, Moazami N, Efimov IR. Conduction remodeling in human end-stage nonischemic left ventricular cardiomyopathy. *Circulation* 2012;125:1835–1847.
- Bonventre JV, Yang L. Kidney injury molecule-1. *Curr Opin Crit Care* 2010;16:556–561.
- Vaidya VS, Ford GM, Waikar SS, Wang Y, Clement MB, Ramirez V, Glaab WE, Troth SP, Sistare FD, Prozialeck WC, et al. A rapid urine test for early detection of kidney injury. *Kidney Int* 2009;76:108–114.
- Dazert E, Hall MN. Mtor signaling in disease. *Curr Opin Cell Biol* 2011;23:744–755.
- Gaut JP, Takasu O, Swanson PE, Hotchkiss RS. Pathology of kidney injury in septic patients. *Mod Pathol* 2012;25:399A.
- Boomer JS, To K, Chang KC, Takasu O, Osborne DF, Walton AH, Bricker TL, Jarman SD II, Kreisel D, Krupnick AS, et al. Immunosuppression in patients who die of sepsis and multiple organ failure. *JAMA* 2011;306:2594–2605.
- Bone RC, Balk RA, Cerra FB, Dellinger RP, Fein AM, Knaus WA, Schein RM, Sibbald WJ. Definitions for sepsis and organ failure and guidelines for the use of innovative therapies in sepsis. The ACCP/SCCM consensus conference committee. American College of Chest Physicians/Society of Critical Care Medicine. *Chest* 1992;101:1644–1655.
- Racusen LC, Solez K, Colvin RB, Bonsib SM, Castro MC, Cavallo T, Croker BP, Demetris AJ, Drachenberg CB, Fogo AB, et al. The banff 97 working classification of renal allograft pathology. *Kidney Int* 1999;55:713–723.
- Watanabe E, Muenzer JT, Hawkins WG, Davis CG, Dixon DJ, McDunn JE, Brackett DJ, Lerner MR, Swanson PE, Hotchkiss RS. Sepsis induces extensive autophagic vacuolization in hepatocytes: a clinical and laboratory-based study. *Lab Invest* 2009;89:549–561.
- Julian MW, Bao S, Knoell DL, Fahy RJ, Shao G, Crouser ED. Intestinal epithelium is more susceptible to cytopathic injury and altered permeability than the lung epithelium in the context of acute sepsis. *Int J Exp Pathol* 2011;92:366–376.

45. Kumar A, Schupp E, Bunnell E, Ali A, Milcarek B, Parrillo JE. Cardiovascular response to dobutamine stress predicts outcome in severe sepsis and septic shock. *Crit Care* 2008;12:R35.
46. Parrillo JE, Burch C, Shelhamer JH, Parker MM, Natanson C, Schuette W. A circulating myocardial depressant substance in humans with septic shock: septic shock patients with a reduced ejection fraction have a circulating factor that depresses in vitro myocardial cell performance. *J Clin Invest* 1985;76:1539–1553.
47. Kumar A, Brar R, Wang P, Dee L, Skorupa G, Khadour F, Schulz R, Parrillo JE. Role of nitric oxide and cgmp in human septic serum-induced depression of cardiac myocyte contractility. *Am J Physiol* 1999;276:R265–R276.
48. Kumar A, Thota V, Dee L, Olson J, Uretz E, Parrillo JE. Tumor necrosis factor alpha and interleukin 1beta are responsible for in vitro myocardial cell depression induced by human septic shock serum. *J Exp Med* 1996;183:949–958.
49. Levy RJ, Deutschman CS. Cytochrome c oxidase dysfunction in sepsis. *Crit Care Med* 2007;35:S468–S475.
50. Celes MR, Torres-Duenas D, Alves-Filho JC, Duarte DB, Cunha FQ, Rossi MA. Reduction of gap and adherens junction proteins and intercalated disc structural remodeling in the hearts of mice submitted to severe cecal ligation and puncture sepsis. *Crit Care Med* 2007;35:2176–2185.
51. Hotchkiss RS, Swanson PE, Freeman BD, Tinsley KW, Cobb JP, Matuschak GM, Buchman TG, Karl IE. Apoptotic cell death in patients with sepsis, shock, and multiple organ dysfunction. *Crit Care Med* 1999;27:1230–1251.
52. Tran M, Tam D, Bardia A, Bhasin M, Rowe GC, Kher A, Zsengeller ZK, Akhavan-Sharif MR, Khankin EV, Saintgeniez M, *et al.* Pgc-1alpha promotes recovery after acute kidney injury during systemic inflammation in mice. *J Clin Invest* 2011;121:4003–4014.
53. Lindgren D, Bostrom AK, Nilsson K, Hansson J, Sjolund J, Moller C, Jirstrom K, Nilsson E, Landberg G, Axelsson H, *et al.* Isolation and characterization of progenitor-like cells from human renal proximal tubules. *Am J Pathol* 2011;178:828–837.
54. Glynn PA, Evans TJ. Inflammatory cytokines induce apoptotic and necrotic cell shedding from human proximal tubular epithelial cell monolayers. *Kidney Int* 1999;55:2573–2597.
55. Hotchkiss RS, Tinsley KW, Swanson PE, Schmiege RE Jr, Hui JJ, Chang KC, Osborne DF, Freeman BD, Cobb JP, Buchman TG, *et al.* Sepsis-induced apoptosis causes progressive profound depletion of B and CD4+ T lymphocytes in humans. *J Immunol* 2001;166:6952–6963.
56. Tenhunen JJ. In death, truth lies: why do patients with sepsis die? *Anesth Analg* 2009;108:1731–1733.
57. Hotchkiss RS, Opal S. Immunotherapy for sepsis: a new approach against an ancient foe. *N Engl J Med* 2010;363:87–89.
58. Pietrangelo M, Macknis J, Hicks S, Zhang P. Kidney injury molecule-1 staining identifies acute tubular injury in pediatric kidneys regardless of autolysis. *Mod Pathol* 2011;24:403A.